



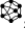



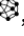


# Effect of operating temperature on the sensor performance of oriented Ni/NiO networks in a PEDOT: PSS matrix for nitrogen dioxide detection

Irek R. Nizameev<sup>ab\*</sup> , Guliya R. Nizameeva<sup>ac</sup> , Viktoria V. Vorobieva<sup>a</sup> ,  
Elgina M. Lebedeva<sup>a</sup>, Oleg G. Sinyashin<sup>a</sup> 

**a:** Arbuzov Institute of Organic and Physical Chemistry , FRC Kazan Scientific Center of RAS, Kazan 420088, Russia

**b:** Department of Nanotechnology in Electronics, Kazan National Research Technical University Named after A.N. Tupolev-KAI , Kazan 420111, Russia

**c:** Department of Physics, Kazan National Research Technological University , Kazan 420015, Russia

\* Corresponding author: [inizameyev@iopc.ru](mailto:inizameyev@iopc.ru)

## Abstract

Given the high ecotoxicity of nitrogen dioxide and its prevalence in urban atmospheres, the development of sensitive sensors for its detection is a pressing task. In this study, a gas-sensitive layer in the form of a composite material based on Ni fibers + NiO nanoparticles embedded in a poly(3,4-ethylenedioxythiophene) polystyrene sulfonate polymer matrix is proposed. The sensor response of the developed material to NO<sub>2</sub> was determined at various operating temperatures. It was found that increasing the operating temperature from 25 to 180 °C leads to a significant increase in the response magnitude and response speed of the sensor to NO<sub>2</sub>. The optimal balance between high sensitivity and long-term signal stability is achieved at a temperature of 120 °C, at which the sensitivity of the material to NO<sub>2</sub> is 6.6·10<sup>-3</sup> ppm<sup>-1</sup>.

## Key findings

- The developed composite sensor exhibits maximum sensitivity to NO<sub>2</sub> at 120 °C, reaching 6.6 × 10<sup>-3</sup> ppm<sup>-1</sup>.
- For the developed material, operating above 60 °C eliminates humidity interference.
- The developed sensor exhibits high selectivity over H<sub>2</sub>S, CO, NH<sub>3</sub>, SO<sub>2</sub>, H<sub>2</sub>, ethanol, and acetone.

© 2026, the Authors. This article is published in open access under the terms and conditions of the Creative Commons Attribution (CC BY) license (<http://creativecommons.org/licenses/by/4.0/>), which permits unrestricted reuse of the work in any medium provided the original work is properly cited.

## Accompanying information

### Article history

Received: 26.03.2026

Revised: 14.04.2026

Accepted: 15.04.2026

Available online: 16.04.2026

### Keywords

Gas sensor; oriented fibers; nickel; nickel oxide; nitrogen dioxide; PEDOT:PSS

### Funding

The reported study was funded by the government assignment for FRC Kazan Scientific Center of RAS

### Supplementary information

Supplementary materials: 

Transparent peer review: 

### Sustainable Development Goals



## 1. Introduction

Due to the continuously increasing pace of industrial growth and the consequent deterioration of the environmental situation, the need to determine the presence and precise concentration of various ecotoxins is also growing [1-4]. Therefore, the development of gas sensors, which are vital in many areas of human activity, is a critical issue. A crucial direction in environmental monitoring is the detection of toxic gases in the atmosphere [5-9].

This work considers a sensor for the highly toxic gas NO<sub>2</sub>, which even at ultra-low concentrations can pose a serious threat to both humans and wildlife. Modern sensors for detecting nitrogen dioxide (NO<sub>2</sub>) are developed based

on various functional materials that serve as the active layer directly responsible for interaction with gas molecules. The most common class of such materials is semiconductor metal oxides, such as tin oxide (SnO<sub>2</sub>), tungsten oxide (WO<sub>3</sub>), zinc oxide (ZnO), etc. [3-7,10]. Their operating principle is based on a change in electrical resistance upon adsorption of NO<sub>2</sub> molecules, which are strong oxidizers, on the material surface. Semiconductor oxides, particularly WO<sub>3</sub>, show high efficiency in NO<sub>2</sub> detection. However, as with most materials of this class, detection requires heating to 200-400 °C, which negatively affects the device's energy efficiency. A more modern alternative is carbon nanomaterials, particularly graphene [11] and carbon nanotubes [12], which can detect NO<sub>2</sub> at room temperature due to

changes in their electrical conductivity upon contact with the gas. However, their surface contains active oxygen-containing groups that act as binding sites for gas molecules. This causes strong adsorption and, consequently, a long recovery time for the sensor. Another alternative is the use of conducting polymers, such as polyaniline or PEDOT:PSS. However, their practical application in gas sensors is hindered by low sensitivity and long response times due to their strong affinity for volatile organic compound molecules and moisture. Combining polymers with inorganic materials is a promising approach for developing gas sensors, which can significantly enhance the selectivity and sensitivity of sensors toward target gases.

The increase in sensitivity achieved by combining inorganic nanomaterials and conducting polymers is associated with several fundamental effects arising from their synergy [13–16]. Such nanostructures possess a large specific surface area, providing numerous active sites for gas molecule adsorption. In turn, polymers often serve as a matrix that prevents agglomeration of these nanostructures, preserving their high surface area accessible to the gas. Another important aspect is that when inorganic nanomaterials are incorporated into a conducting polymer matrix, depending on the nature of the inorganic phase, a *p-n* junction or a Schottky barrier forms at the interface between the conducting polymer and the inorganic material [17–21]. Such a heterojunction acts as an energy barrier, and gas molecules adsorbing on the material can alter the width of this barrier. To date, numerous nanocomposite materials of the "polymer + inorganic phase" type have been developed for use as sensitive elements in sensors. Nanocomposites of polyaniline with metal-metal oxide nanorod complexes demonstrate good sensitivity and selectivity toward various toxic gases, including NO<sub>2</sub> [22,23]. Polypyrrole and its composites are also promising materials for developing nitrogen dioxide sensors capable of effectively detecting this toxic gas at room temperature [24–27].

Another important class of conducting polymers promising for creating composite sensing elements in gas sensors (including nitrogen dioxide sensors) are polythiophenes and their derivatives, such as poly(3,4-ethylenedioxythiophene) (PEDOT) and PEDOT:PSS. Owing to their high chemical and thermal stability, good solubility in many solvents, and high conductivity in the doped state, polythiophenes have become a key component of composite sensing elements in nitrogen dioxide sensors [28–32]. Although composites based on conducting polymers demonstrate significant potential for developing gas sensors, their ultimate effectiveness depends on the morphology and degree of dispersion of the system. The best results are shown by composite materials where the inorganic phase is structured in the form of nanoparticles [33], nanowires [34], or porous structures uniformly distributed within the polymer matrix. As of now, a literature analysis using an international database of articles shows that out of more than 8500 pub-

lications on NO<sub>2</sub> sensors, only about 320 focus on interdigitated electrodes and approximately 115 on resistive or chemiresistive PEDOT:PSS-based or NiO-based materials, confirming that this specific combination represents a much narrower research niche.

Previously, we developed a gas-sensitive material for an NO<sub>2</sub> sensor based on the NiFs-NiO-PEDOT:PSS structure [35,36]. The base of the material is an oriented network of nickel fibers with a highly developed surface. The top layer of the network is covered with a layer of nickel oxide. The entire network is embedded in a polymer matrix of poly(3,4-ethylenedioxythiophene) polystyrene sulfonate (PEDOT:PSS). We were able to demonstrate that such a structure exhibits good sensitivity to NO<sub>2</sub> in air even at room temperature. However, at room temperature, for this type of gas sensor, there is an effect of air humidity influencing the sensor response. For accurate calibration of the response, this effect must be taken into account. In this work, we investigated the influence of the operating temperature of the developed sensor on its characteristics: the effect of air humidity, response and recovery rates, response magnitude, and sensitivity.

## 2. Experimental

All used reagents were commercially available and were used as purchased. The chemicals nickel chloride (NiCl<sub>2</sub>·6H<sub>2</sub>O), hydrazine hydrate (N<sub>2</sub>H<sub>5</sub>OH), poly(3,4-ethylenedioxythiophene) polystyrene sulfonate (PEDOT:PSS), ethylene glycol (EG), and isopropyl alcohol (IPA) were from Sigma-Aldrich.

The method for the synthesis of the composite material is described in detail in our previous works [35,36]. Briefly, the method consists of three main stages: synthesis of nickel fibers; structuring of the fibers into an anisotropic network using a magnetic field; partial thermal oxidation of the surface layer of the fibers (the importance of incomplete nickel oxidation and its procedure are discussed in more detail in our work [37]); and application of a thin film of PEDOT:PSS (0.3% Sigma Aldrich) to the surface of the oxidized fibers.

Scanning electron microscopy (SEM) and energy-dispersive X-ray spectroscopy (EDS) studies were performed using a Carl Zeiss EVO 50 XVP microscope (HV = 20 kV, WD = 9 mm) (Germany).

Gas sensitivity and sensor characteristic studies were conducted in a specialized gas-tight stainless steel chamber, into which gas was supplied from a cylinder containing a certified reference gas mixture with a known content of the target gas. The state of the gas mixture in the chamber was monitored and regulated using an IKA Vacstar Digital system with a VC 10 pro controller, IKA (Germany). The pressure in the chamber was maintained at 100 ± 10 kPa. The current-voltage characteristics of the sensor were measured using a P-45X potentiostat-galvanostat (Electrochemical Instruments, Russia). The resistance of the sensor was

determined by measuring the electrical current at a constant applied voltage of 100 mV. The current was recorded in real time, and the resistance was calculated using Ohm's law. No external current was imposed independently.

To fabricate the interdigitated electrode (IDE) sensor, gold electrodes were deposited onto a glass substrate. The electrodes were deposited using UV photolithography and magnetron sputtering (C156RS sputtering system, Russia). Magnetron sputtering of the gold electrodes was carried out in an argon atmosphere.

### 3. Results and discussion

Previously, we developed a method for producing a gas-sensitive material that responds to the presence of nitrogen dioxide in air, based on a composite material in the form of a network of nickel oxide fibers coated with nickel oxide and embedded in a PEDOT:PSS polymer matrix [35,36]. To test the sensor characteristics of the studied material, it is necessary to transfer it onto a substrate with electrodes, i.e., to implement it as a so-called IDE sensor (IDE – interdigitated electrodes). In this work, the IDE sensor is implemented as a system of gold electrodes on the surface of silicate glass with the sensitive material deposited in the center (Figure 1).

The material exhibits a morphology comprising a network of nickel fibers with a developed surface. The fibers are coated with an NiO layer and embedded in a PEDOT:PSS polymer matrix (Figure 2).

The active component material exhibits semiconducting electrical conductivity (*p*-type semiconductor). In *p*-type semiconductors, electrons are minority charge carriers, and a decrease in their number in the near-surface layer due to chemisorption of nitrogen dioxide molecules causes a noticeable change in the resistance of the conduction channel of the layer as a whole. This mechanism is used to detect the presence and determine the amount of NO<sub>2</sub> molecules in the air. PEDOT:PSS possesses sufficient electrical conductivity and ensures the structural stability of the polymer-metal-semiconductor composite material. This system is denoted as *NiFs-NiO-PEDOT:PSS*. The elemental composition of the material was confirmed by energy-dispersive X-ray spectroscopy (the spectrum is shown in Figure 2). In the EDS spectrum, peaks corresponding to nickel (K $\alpha$  = 7.48 keV, K $\beta$  = 8.27 keV), oxygen (K $\alpha$  = 0.53 keV), carbon (K $\alpha$  = 0.28 keV), and sulfur (K $\alpha$  = 2.31 keV) are clearly visible. The partial oxidation of nickel fibers was performed according to the protocol established in [37], where EDS and XRD confirmed a Ni:NiO ratio of 4:1. While the NiO layer thickness may influence the NiO/PEDOT:PSS junction, the controlled conditions ensure reproducibility. A systematic study of thickness effects is planned for future investigations.

Tests have shown that the developed material exhibits sensitivity to nitrogen dioxide even at its relatively low concentrations in air (50 ppm NO<sub>2</sub>). Under certain conditions

in laboratory tests, the sensor response of the material occurs even at room temperature. However, it should be borne in mind that under real-world detection conditions, the sensor response is affected by air humidity [38]. In this study, work was carried out to select the optimal operating temperature of the developed sensor at which a high sensor response is observed, and the influence of air humidity is minimal.

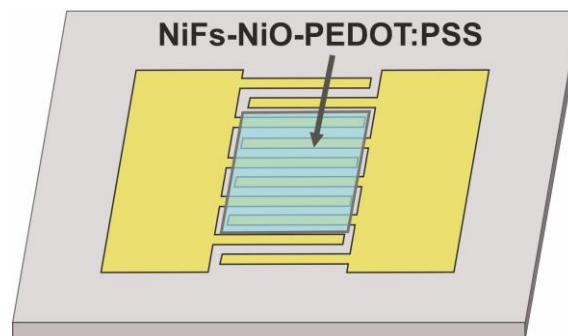


Figure 1 Schematic representation of the sensor active element (IDE sensor).

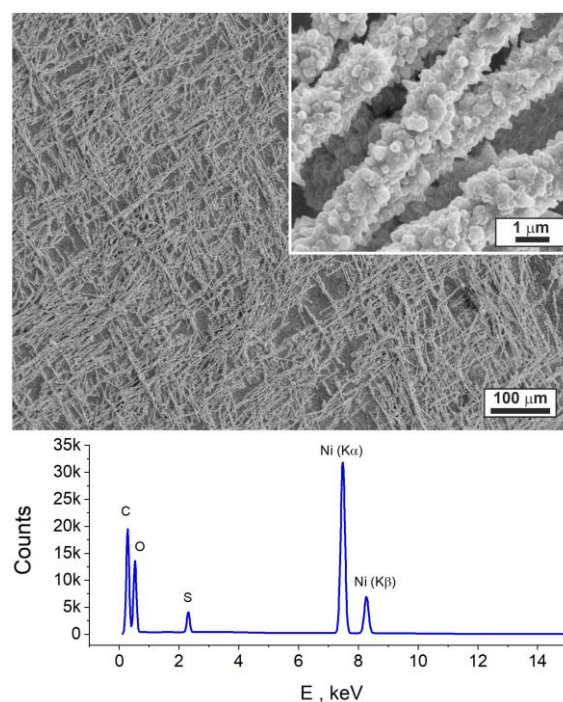


Figure 2 SEM images of the morphology of the *NiFs-NiO-PEDOT:PSS* material and the corresponding energy-dispersive X-ray spectroscopy (EDS) spectrum.

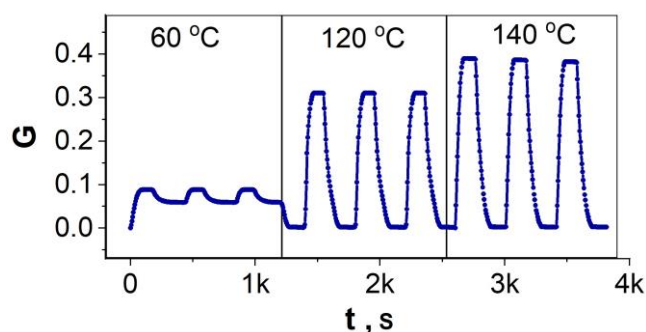


Figure 3 Sensor response of *NiFs-NiO-PEDOT:PSS* to NO<sub>2</sub> (50 ppm) at different temperatures.

To investigate the sensor characteristics, the IDE sensor with the developed **NiFs-NiO-PEDOT:PSS** gas-sensitive material was placed in a sealed chamber with a sealed electrical feedthrough and an inlet valve for creating a vacuum or an atmosphere with a known gas composition. For chemoresistive types of sensors, the operating temperature is important because the sensor response may depend on it. The sensor response, expressed in relative units, is calculated according to the formula:

$$G = |R_{\text{gas}} - R_0| / R_0, \quad (1)$$

where  $R_{\text{gas}}$  is the sensor resistance in the presence of the test gas, and  $R_0$  is the sensor resistance before exposure to the test gas. In addition to the sensor response, in practice, the response time  $\tau_{0.9}$  is used as a parameter characterizing the speed of response of a gas sensor. This is the time required for the sensor to reach 90% of the  $G$  value corresponding to the given conditions. Along with the response time, the sensor recovery time  $\tau_{\text{rec}}$  is also considered. This parameter characterizes the decay time of the sensor response pulse after the removal of the target gas.

Measurements were carried out at temperatures ranging from 25 to 180 °C. Figure 3 illustrates how the sensor signal changes upon exposure to 50 ppm of nitrogen dioxide in an air environment as a function of the set temperature.

A clear dependence of the sensor response magnitude on the operating temperature is observed: as the temperature increases, the signal increases. Thus, increasing the temperature from 60 to 140 °C leads to an increase in the sensor response  $G$  upon exposure to 50 ppm  $\text{NO}_2$  from 0.088 to 0.390. Concurrently, the kinetic parameters of the sensor operation change: the response time ( $\tau_{0.9}$ ) and the recovery time ( $\tau_{\text{rec}}$ ) decrease (Table 1). This indicates an acceleration of the interaction processes between the sensor and the target gas ( $\text{NO}_2$ ). The change in the sensor signal shape with increasing temperature is shown in Figure 4.

In the temperature range below 60 °C, the **NiFs-NiO-PEDOT:PSS** composite material exhibits incomplete recovery of the initial signal (Figure 5). This effect is likely due to incomplete desorption of the target gas molecules and the competitive influence of water vapor adsorption from the air [38].

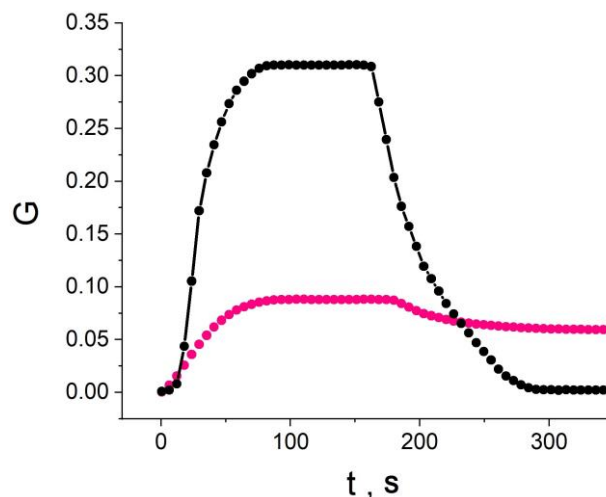
As noted in the literature, at temperatures below 100 °C, a slight baseline drift may be observed due to slow and incomplete desorption of  $\text{NO}_2$ , as a result of which the recovery time ( $\tau_{\text{rec}}$ ) can reach thousands of seconds [38].

The response impulses for most temperatures are qualitatively similar and differ only in amplitude, except for the measurements at 60 °C, which exhibit a distinct behavior. The response values for all investigated temperatures are fully presented in Figure 6, which summarizes the sensitivity and response magnitude across the entire temperature range.

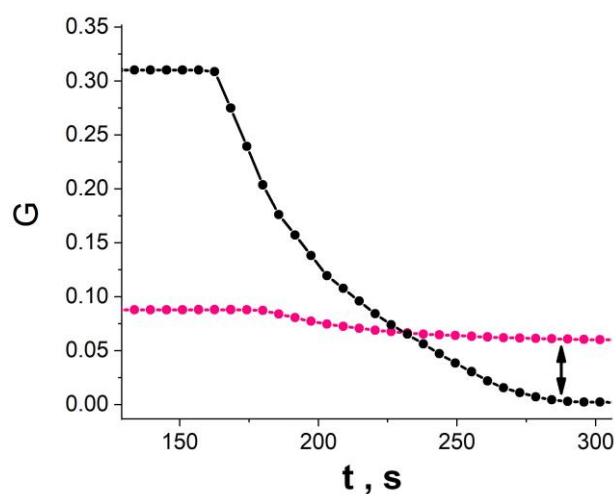
In this work, the temperature dependence of the sensor response was studied in the range of 25–180 °C (Figure 6).

A monotonic increase in the sensor response  $G$  with increasing temperature is observed, with its value exceeding 0.5 at 180 °C. For comparison, Figure 6 also shows data for unmodified PEDOT:PSS, which indicate that the incorporation of NiFs-NiO into the composite leads to a significant increase in the sensitivity of the material.

However, it was found that at temperatures above 140 °C, the sensor stability deteriorates (Figure 7): a decrease in the response is observed during prolonged measurements.



**Figure 4** Sensor response pulse to 50 ppm nitrogen dioxide at 60 °C (red line) and 120 °C (black line).



**Figure 5** Recovery region of the response pulse at 60 °C (red line) and 120 °C (black line).

**Table 1** Response parameters of the **NiFs-NiO-PEDOT:PSS** sensor as a function of temperature.

$t$ (°C)	$\tau_{0.9}$ (s)	$\tau_{\text{rec}}$ (s)
40	$90 \pm 5$	>1000
60	$90 \pm 5$	>1000
100	$90 \pm 5$	$360 \pm 10$
120	$90 \pm 5$	$230 \pm 10$
140	$70 \pm 3$	$120 \pm 10$
160	$50 \pm 3$	$110 \pm 10$
180	$45 \pm 5$	$70 \pm 10$

This effect is explained by an increase in the electrical resistance of the material. In our observations, at temperatures above 140 °C, an irreversible increase in the material resistance is observed. This is primarily attributed to the thermo-oxidative degradation of PEDOT:PSS. We expected this process to occur in our work. What was important for us was to determine that the thermo-oxidative degradation of PEDOT:PSS takes place at temperatures higher than those required to eliminate the humidity effect on the detected gas. Thus, based on an analysis of the response and its stability, the optimal operating temperature was determined to be 120 °C. At this temperature, a high and temporally stable sensor signal is achieved (Figure 7).

The sensor response of *NiFs-NiO-PEDOT:PSS* depends almost linearly on the NO<sub>2</sub> concentration in the gas mixture in the concentration range of 1–100 ppm (Figure 8). Over the 1–100 ppm range, the response is approximately linear (correlation coefficient  $R^2 \approx 0.98$ ), which is why the single sensitivity value  $S$  is often used in the literature for comparative purposes. The sensor sensitivity in this case can be determined from the slope of the graph:

$$S = \Delta G / \Delta C, \quad (2)$$

where  $C$  is the nitrogen dioxide concentration.

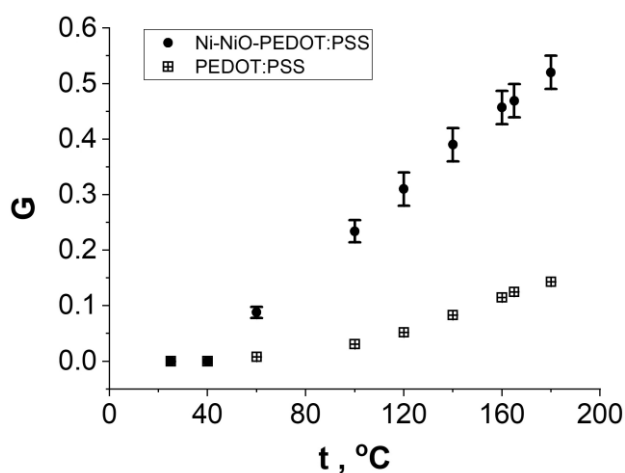


Figure 6 Temperature dependence of the sensor response for *NiFs-NiO-PEDOT:PSS* and for pure PEDOT:PSS.

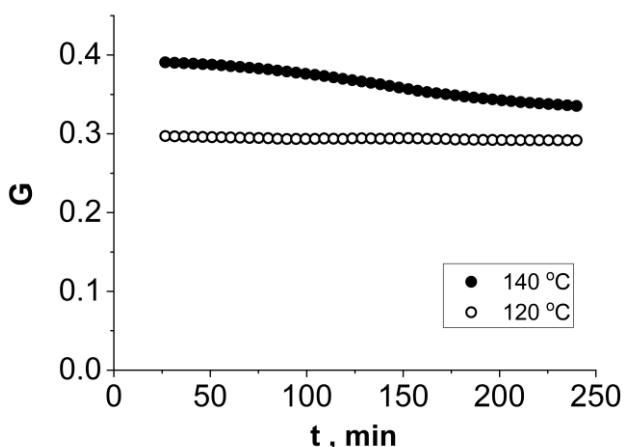


Figure 7 Long-term sensor response stability of *NiFs-NiO-PEDOT:PSS*.

For the *NiFs-NiO-PEDOT:PSS* material, the sensitivity  $S$  of the sensor to NO<sub>2</sub> at a temperature of 120 °C was  $(6.6 \pm 0.4) \times 10^{-3} \text{ ppm}^{-1}$ . A comparison of the sensing behavior of the present material with previously reported data is presented in Table 2.

The effect of relative humidity (RH) of the ambient atmosphere on the sensor characteristics was investigated. The measurement results of the *NiFs-NiO-PEDOT:PSS* response in the humidity range of 20–80% are shown in Figure 9.

Table 2 Comparison of NO<sub>2</sub> sensing behavior of the *NiFs-NiO-PEDOT:PSS* sensor with previously reported data.

Sample	t, °C	C(NO <sub>2</sub> ), ppm	G, %	Ref.
Graphene	RT	5	12	[39]
Graphene / MoS <sub>2</sub>	150 °C	5	7	[40]
TiO <sub>2</sub>	RT	100	2.4	[41]
SnO <sub>2</sub> /CuO	100 °C	1	68	[38]
RGO	RT	100 (5)	83 (4.1)	[42]
Ce <sub>2</sub> Sn <sub>2</sub> O <sub>7</sub> / CNFs	25 °C	2	20	[4]
PEDOT:PSS / Ti <sub>3</sub> C <sub>2</sub> T <sub>x</sub> /ZnO	24 °C	1	10	[28]
PEDOT:PSS / ZnO	24 °C	1	0.7	[28]
Polypyrrole / RGO	25 °C	5	5	[26]
Polypyrrole	25 °C	100	36	[43]
NiFs-NiO-PEDOT:PSS	120 °C	100 (5)	66 (3.2)	This work

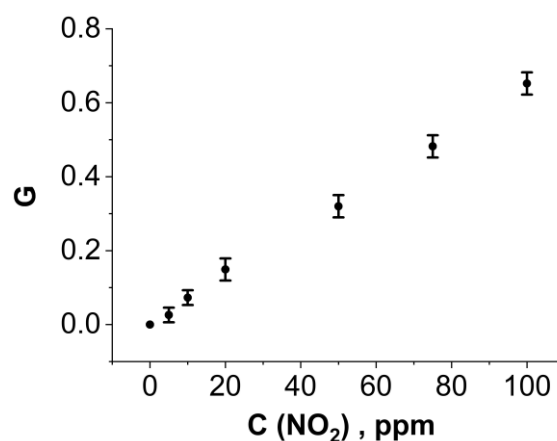


Figure 8 Dependence of the sensor response of *NiFs-NiO-PEDOT:PSS* on nitrogen dioxide concentration at an operating temperature of 120 °C.

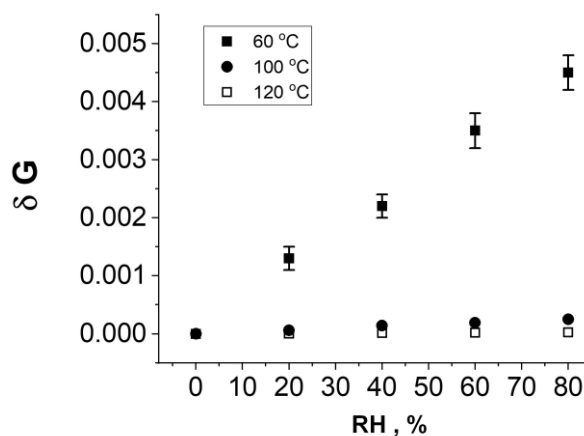
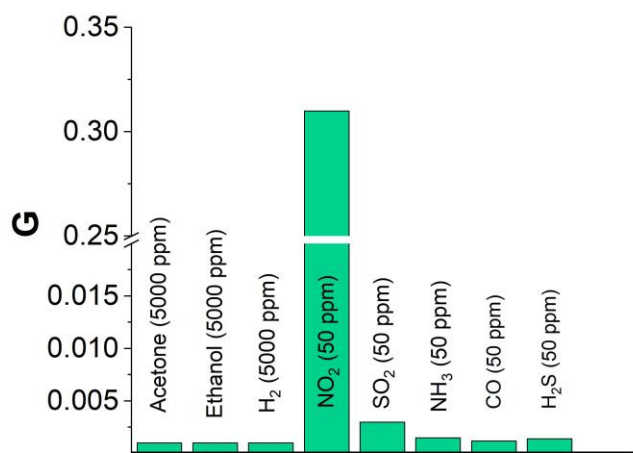


Figure 9 Change in the sensor response of *NiFs-NiO-PEDOT:PSS* upon increasing the relative humidity of the test gas mixture containing air and nitrogen dioxide.



**Figure 10** Selectivity of the sensor response of *NiFs-NiO-PEDOT:PSS*.

As can be seen, the change in the sensor response  $\delta G$  increases with increasing relative humidity. In this case, this value is negative and corresponds to a decrease in the response. This decrease in sensitivity is likely due to competitive adsorption of water molecules, which block the active sites on the material surface intended for interaction with  $\text{NO}_2$ . In addition, water molecules can cause swelling of the PEDOT:PSS matrix, alter the interchain distance, change the dielectric environment, and influence hopping transport between PEDOT-rich domains. These effects are separate from competitive adsorption with analyte gases. The most significant suppressing effect of humidity is observed in the low-temperature region (25–60 °C). At operating temperatures above 60 °C, the contribution of humidity to the sensor response of the *NiFs-NiO-PEDOT:PSS* composite becomes negligible.

The developed sensitive material demonstrates high selectivity of response to nitrogen dioxide. To determine the cross-selectivity of the sensor response of *NiFs-NiO-PEDOT:PSS*, tests were conducted in various gas mixtures containing major greenhouse/hazardous gases, Figure 10.

The cross-selectivity of the sensor response to nitrogen dioxide is numerically characterized by the value  $K(\text{NO}_2) = G(\text{NO}_2) / G(X)$ , where  $G(X)$  is the response to another gas. We tested the sensor properties of *NiFs-NiO-PEDOT:PSS* in the presence of the following gases in the gas mixture:  $\text{H}_2\text{S}$ ,  $\text{CO}$ ,  $\text{NH}_3$ ,  $\text{SO}_2$ ,  $\text{H}_2$ , ethanol vapor, and acetone vapor. When the material interacts with oxidizing and reducing gases, the response has opposite signs. For example, upon interaction with  $\text{NO}_2$ , chemisorption processes lead to a decrease in the concentration of free electrons (which are not the majority carriers for p-type semiconductors). For p-type semiconductors, this causes an increase in electrical conductivity. When investigating the response of the developed material to different types of gases, we observed a decrease in resistance upon exposure to oxidizing gases and an increase in resistance upon exposure to reducing gases. However, for simplicity and ease of interpreta-

tion, the work uses the absolute value of the sensor response  $\Delta G$ , as indicated in Equation (1). For all gases studied, the  $K(\text{NO}_2)$  value significantly exceeds 100.

#### 4. Limitations

This work did not investigate the effect of the amount of PEDOT:PSS polymer used on the sensor characteristics. It is assumed that the main contribution to the studied properties comes from the Ni–NiO fiber network.

Another limitation of the present study is that we did not perform a systematic analysis of the NiO layer thickness on the nickel fibers or its influence on the NiO/PEDOT:PSS junction behavior. While the controlled oxidation conditions ensured reproducibility across different samples, and the Ni:NiO ratio was verified to be approximately 4:1 using EDS and XRD [37], the exact thickness of the NiO layer remains unknown. A thicker NiO layer could potentially widen the depletion region at the NiO/PEDOT:PSS interface and affect charge transfer efficiency. Future work should employ high-resolution techniques such as transmission electron microscopy or X-ray photoelectron spectroscopy depth profiling to correlate NiO layer thickness with junction properties and overall sensor performance.

EDS elemental mapping was not performed due to technical limitations of the available SEM (lack of a dedicated scanning system for EDS mapping). While such mapping would provide additional spatial distribution information, the present EDS point analysis (Figure 2) confirms the presence of the expected elements. Future work using appropriate instrumentation should address this point.

We did not quantitatively separate the contribution of water-induced swelling of PEDOT:PSS from competitive adsorption effects on the humidity response. While both mechanisms are suppressed at elevated temperatures, their individual roles below 60 °C require further investigation using, for example, operando ellipsometry or quartz crystal microbalance measurements.

Long-term stability under real operating conditions has not yet been systematically evaluated. The sensor performance may degrade over time due to prolonged exposure to humidity, temperature fluctuations, and aging effects of the PEDOT:PSS matrix or the Ni/NiO surface. Accelerated aging tests and continuous operation studies are needed to assess the practical lifetime of the sensor.

Batch-to-batch reproducibility of the *NiFs-NiO-PEDOT:PSS* composite has not been quantitatively assessed. Although the synthesis protocol was kept consistent, variations in fiber oxidation, PEDOT:PSS distribution, or film thickness between different preparation runs may affect sensor performance. Future work should include statistical analysis across multiple independent batches.

## 5. Conclusions

As a result of the conducted studies, the optimal operating conditions for the sensor based on the **NiFs-NiO-PEDOT:PSS** composite material were determined. It was established that increasing the operating temperature from 25 to 180 °C leads to a significant increase in the amplitude and response speed to NO<sub>2</sub>. The kinetic parameters ( $\tau_{0.9}$  and  $\tau_{rec}$ ) decrease, indicating an acceleration of the gas adsorption-desorption processes. The best balance between high sensitivity and long-term signal stability is achieved at a temperature of 120 °C. At this value, the maximum sensitivity (*S*) of the material to NO<sub>2</sub> was recorded, amounting to  $6.6 \times 10^{-3}$  ppm<sup>-1</sup>. Furthermore, under this temperature regime, the influence of relative air humidity on the sensor operation becomes negligible. The developed material demonstrates high selectivity of response to nitrogen dioxide. For all gases studied, the *K*(NO<sub>2</sub>) value significantly exceeds 100.

### Supplementary materials

No supplementary materials are available.

### Data availability statement

The raw/processed data required to reproduce the above findings cannot be shared at this time as the data also forms part of an ongoing study.

### Acknowledgments

None.

### Author contributions

Conceptualization: G.R.N., I.R.N., O.G.S.

Data curation: G.R.N., I.R.N.

Formal Analysis: G.R.N., I.R.N.

Funding acquisition: I.R.N.

Investigation: V.V.V., E.M.L., G.R.N.

Methodology: I.R.N., G.R.N., V.V.V., E.M.L., O.G.S.

Project administration: I.R.N.

Resources: G.R.N., I.R.N.

Software: G.R.N., I.R.N.

Supervision: I.R.N., O.G.S.

Validation: G.R.N., I.R.N.

Visualization: V.V.V., G.R.N., I.R.N.

Writing – original draft: G.R.N., I.R.N., O.G.S.

Writing – review & editing: G.R.N., I.R.N., O.G.S.

(Irek R. Nizameev = I.R.N.; Guliya R. Nizameeva = G.R.N.; Viktoria V. Vorobieva = V.V.V.; Elgina M. Lebedeva = E.M.L.; Oleg G. Sinyashin = O.G.S.)

### Conflict of interest

The authors declare no conflict of interest.

### Additional information

Author IDs:

Irek R. Nizameev, Scopus ID [35799942900](https://orcid.org/0000-0002-3579-9942);

Guliya R. Nizameeva, Scopus ID [57204606299](https://orcid.org/0000-0002-5720-4606);

Viktoria V. Vorobieva, Scopus ID [59421978800](https://orcid.org/0000-0002-5942-1978);

Elgina M. Lebedeva, Scopus ID [58568898200](https://orcid.org/0000-0002-5856-8898);

Oleg G. Sinyashin, Scopus ID [57188848065](https://orcid.org/0000-0002-5718-8848).

## References

- Aminov S V, Fedotov V V, Kopchuk D S, Kudryashova E A, Sayfutdinova Y M, Moseev T D, Varaksin M V, Tsmokalyuk A N, Zyryanov G V, Rusinov V L. Sodium salts of 6-hydroxy-azolo[1,5-a]pyrimidine-5-carbonitriles as red-emissive fluorescent chemosensors for picric acid. *Chimica Techno Acta*. 2026;13(2):9537. doi:10.15826/chimtech.9537
- Kappo D, Stoikov D I, Stoikov D I, Karaguzina K R, Shurpik D N, Stoikov I I, Evtugyn G A. Voltammetric sensor based on electropolymerized poly(Neutral Red) and pillar[3]arene[2]hydroquinone ammonium derivative for dopamine and ascorbic acid determination. *Chimica Techno Acta*. 2025;12(1):02. doi:10.15826/chimtech.2025.12.1.02
- Kalyakin A S, Volkov A N. Electrochemical detection of simple alkanes by utilizing a solid-state zirconia-based gas sensor. *Chimica Techno Acta*. 2023;10(1):09. doi:10.15826/chimtech.2023.10.1.09
- Al-Ithawi W K A, Baklykov A V, Platonov V A, Ballou Y, Pokharkar O, Khasanov A F, Kovalev I S, Nikonov I L, Kopchuk D S, Samigullina R F, Shafran Y M, Belyaev N A, Zyryanov G V. Mechano-synthesis of equol-based polycarbonate and polyester as chemosensors for detection of nitro-explosives. *Chimica Techno Acta*. 2025;12(3):12306. doi:10.15826/chimtech.2025.12.3.06
- Aparnev A I, Loginov A V, Bannov A G, Novgorodtseva O N, Shishin A A. Ce<sub>2</sub>Sn<sub>2</sub>O<sub>7</sub>/CNFs composite as a material for gas sensors and supercapacitors. *Chimica Techno Acta*. 2025;12(4):9052. doi:10.15826/chimtech.9052
- Wang W, Cao J, Wang D, Zhang R, Zhang Y, Zhao L. Insight into SnO<sub>2</sub>-based gas-sensitive materials and readout circuits for semiconductor gas sensors. *Nano Materials Science*. 2025. (In Press) doi:10.1016/j.nanoms.2024.10.012
- Jiang B, Zhou T, Zhang L, Yang J, Han W, Sun Y, Liu F, Sun P, Zhang H, Lu G. Separated detection of ethanol and acetone based on SnO<sub>2</sub>-ZnO gas sensor with improved humidity tolerance. *Sensors and Actuators B: Chemical*. 2023;393:134257. doi:10.1016/j.snb.2023.134257
- Yang T, Boepple M, Hémercyck A, Jay A, Karwounopoulos S, Weimar U, Barsan N. H<sub>2</sub>S Sensing with SnO<sub>2</sub>-Based Gas Sensors: Sulfur Poisoning Mechanism Revealed by Operando DRIFTS and DFT Calculations. *Angewandte Chemie International Edition*. 2025;64(23):e202504696. doi:10.1002/anie.202504696
- Mathankumar G, Harish S, Mohan MK, Bharathi P, Kannan SK, Archana J, Navaneethan M. Enhanced selectivity and ultra-fast detection of NO<sub>2</sub> gas sensor via Ag modified WO<sub>3</sub> nanostructures for gas sensing applications. *Sensors and Actuators B: Chemical*. 2023;381:133374. doi:10.1016/j.snb.2023.133374
- Umar A, Akbar S, Kumar R, Amu-Darko JNO, Hussain S, Ibrahim AA, Alhamami MA, Almebad N, Almas T, Seliem AF. Ce-doped ZnO nanostructures: A promising platform for NO<sub>2</sub> gas sensing. *Chemosphere*. 2024;349:140838. doi:10.1016/j.chemosphere.2023.140838
- Recum P, Hirsch T. Graphene-based chemiresistive gas sensors. *Nanoscale Advances*. 2024;6(1):11-31. doi:10.1039/D3NA00723E
- Pagidi S, Pasupuleti KS, Reddeppa M, Ahn S, Kim Y, Kim JH, Kim MD, Lee SH, Jeon MY. Resistive type NO<sub>2</sub> gas sensing in polymer-dispersed liquid crystals with functionalized-carbon nanotubes dopant at room temperature. *Sensors and Actuators B: Chemical*. 2022;370:132482. doi:10.1016/j.snb.2022.132482
- Karmakar N, Jain S, Fernandes R, Shah A, Patil U, Shimpi N, Kothari D. Enhanced sensing performance of an ammonia gas sensor based on Ag-decorated ZnO nanorods/polyaniline nanocomposite. *ChemistrySelect*. 2023;8(18):e202204284. doi:10.1002/slct.202204284

14. Kausar A. Technological sway of polymer and nanoflower nanofiller consequent nanocomposite—state-of-the-art. *Polymer-Plastics Technology and Materials*. 2021;60(18):2057-2074. [doi:10.1080/25740881.2021.1934015](https://doi.org/10.1080/25740881.2021.1934015)
15. Bonyani M, Zebarjad SM, Janghorban K, Kim JY, Kim HW, Kim SS. Au-decorated polyaniline-ZnO electrospun composite nanofiber gas sensors with enhanced response to NO<sub>2</sub> gas. *Chemosensors*. 2022;10(10):388. [doi:10.3390/chemosensors10100388](https://doi.org/10.3390/chemosensors10100388)
16. Khalifa M, Anandhan S. Highly sensitive and wearable NO<sub>2</sub> gas sensor based on PVDF nanofabric containing embedded polyaniline/g-C<sub>3</sub>N<sub>4</sub> nanosheet composites. *Nanotechnology*. 2021;32(48):485504. [doi:10.1088/1361-6528/ac1e1a](https://doi.org/10.1088/1361-6528/ac1e1a)
17. Tran VV, Nu TTV, Jung HR, Chang M. Advanced photocatalysts based on conducting polymer/metal oxide composites for environmental applications. *Polymers*. 2021;13(18):3031. [doi:10.3390/polym13183031](https://doi.org/10.3390/polym13183031)
18. Thomas SW, Khan RR, Puttananjegowda K, Serrano-Garcia W. Conductive polymers and metal oxide polymeric composites for nanostructures and nanodevices. In: *Advances in Nanostructured Materials and Nanopatterning Technologies*. Elsevier; 2020. p. 243-271. [doi:10.1016/B978-0-12-820055-1.00009-8](https://doi.org/10.1016/B978-0-12-820055-1.00009-8)
19. Im S, Kim S, Kim S, Kim FS, Kim JH. A study on improving electrical conductivity for conducting polymers and their applications to transparent electrodes. *Applied Chemistry for Engineering*. 2015;26(6):640-647. [doi:10.14478/ace.2015.1104](https://doi.org/10.14478/ace.2015.1104)
20. Sarangi AK, Tripathy L, Ansari A, Mohapatra RK, Bhoi SK. Enhancing conductivity in polymers: The role of metal ions in conducting polymer systems. *Polymers for Advanced Technologies*. 2024;35(7):e6505. [doi:10.1002/pat.6505](https://doi.org/10.1002/pat.6505)
21. Shahrim NAA, Ahmad Z, Azman AW, Buys YF, Sarifuddin N. Mechanisms for doped PEDOT: PSS electrical conductivity improvement. *Materials Advances*. 2021;2(22):7118-7138. [doi:10.1039/D1MA00690A](https://doi.org/10.1039/D1MA00690A)
22. Murugesan T, Kumar RR, Anbalagan AK, Lee CH, Lin HN. Interlinked polyaniline/ZnO nanorod composite for selective NO<sub>2</sub> gas sensing at room temperature. *ACS Applied Nano Materials*. 2022;5(4):4921-4930. [doi:10.1021/acsnam.1c04519](https://doi.org/10.1021/acsnam.1c04519)
23. Umar A, Ibrahim AA, Algadi H, Albargi H, Alsairi MA, Wang Y, Akbar S. Enhanced NO<sub>2</sub> gas sensor device based on supramolecularly assembled polyaniline/silver oxide/graphene oxide composites. *Ceramics International*. 2021;47(18):25696-25707. [doi:10.1016/j.ceramint.2021.05.292](https://doi.org/10.1016/j.ceramint.2021.05.292)
24. Dong VT, Hung PT, Anh LD, Vuong LQ, Khanh DD, Huong NT. Zinc Oxide/Polypyrrole particle-decorated rod structure for NO<sub>2</sub> detection at low temperature. *Vietnam Journal of Science and Technology*. 2023. [doi:10.15625/2525-2518/18528](https://doi.org/10.15625/2525-2518/18528)
25. Zhao K, Shi Y, Cui M, Tang B, Zheng C, Chen Q, Hu Y. Flexible Resistive Gas Sensor Based on Molybdenum Disulfide-Modified Polypyrrole for Trace NO<sub>2</sub> Detection. *Polymers*. 2024;16(13):1940. [doi:10.3390/polym16131940](https://doi.org/10.3390/polym16131940)
26. Guettiche D, Mekki A, Debiemme-Chouvy C, Simon N, Sayah ZBD, Tighilt FZ, Touijine S, Mansri O. One-step electro-synthesis of a nanocomposite of functionalized graphene and polypyrrole for enhanced room-temperature nitrogen oxide sensing. *Journal of Polymer Science*. 2024;62(23):5317-5331. [doi:10.1002/pol.20240269](https://doi.org/10.1002/pol.20240269)
27. Saleh WR, Taradh AY, Hassan SM, Ibrahim FT. Flexible NO<sub>2</sub> Gas Sensor Based on Functionalized MWCNTs Modified with a Layer of Metallic Nanoparticles and Polypyrrole Conductive Polymer Works at Room Temperature. *Journal of Nano Research*. 2025;87:21-31. [doi:10.4028/p-d44Y78](https://doi.org/10.4028/p-d44Y78)
28. Tseng SF, Lin YH, Zhou MH, Hsu SH, Hsiao WT. Synthesis of Ti<sub>3</sub>C<sub>2</sub>Tx/ZnO composites decorated with PEDOT: PSS for NO<sub>2</sub> gas sensors. *The International Journal of Advanced Manufacturing Technology*. 2023;126(5):2269-2281. [doi:10.1007/s00170-023-11285-5](https://doi.org/10.1007/s00170-023-11285-5)
29. Wuloh J, Agorku ES, Boadi NO. Modification of metal oxide semiconductor gas sensors using conducting polymer materials. *Journal of Sensors*. 2023;2023(1):7427986. [doi:10.1155/2023/7427986](https://doi.org/10.1155/2023/7427986)
30. Shirgaonkar DB, Yewale MA, Shin DK, Mathad SN, Nakate UT, Ahmad R, Pawar SD, Al-Kantani AA, Aftab S. High selectivity in NO<sub>2</sub> gas sensing applications using polythiophene-MnO<sub>2</sub> composite thin films. *Sensors and Actuators A: Physical*. 2024;377:115740. [doi:10.1016/j.sna.2024.115740](https://doi.org/10.1016/j.sna.2024.115740)
31. Farea MA, Yusof N, Mohammed HY, Murshed MN, Samir A, Hendi A, Osman AM. Enhanced NO<sub>2</sub> sensing performance of CdS nanoparticle-modified PEDOT: PSS composite: a systematic study of ultrasensitivity and reliability. *Colloids and Surfaces A: Physicochemical and Engineering Aspects*. 2024;703:135305. [doi:10.1016/j.colsurfa.2024.135305](https://doi.org/10.1016/j.colsurfa.2024.135305)
32. Dutta P, Sharma A, Kumar V, Gupta G. Ultrasensitive NO<sub>2</sub> Gas Sensor at Room Temperature Based on a Glycerol-Cross-Linked PEDOT: PSS-MoS<sub>2</sub> Nanocomposite. *ACS Applied Polymer Materials*. 2024;7(1):94-105. [doi:10.1021/acscapm.4c02933](https://doi.org/10.1021/acscapm.4c02933)
33. Kausar A, Ahmad I, Zhao T, Aldaghi O, Ibnaouf KH, Eisa MH. Multifunctional polymeric nanocomposites for sensing applications—design, features, and technical advancements. *Crystals*. 2023;13(7):1144. [doi:10.3390/cryst13071144](https://doi.org/10.3390/cryst13071144)
34. Khan E. Polymer nanocomposites for sensing applications. In: *Smart Polymer Nanocomposites*. Elsevier; 2023. p. 305-331. [doi:10.1016/B978-0-323-91611-0.00003-7](https://doi.org/10.1016/B978-0-323-91611-0.00003-7)
35. Nizameeva G R, Kuznetsova V V, Lebedeva E M, Ivanova A A, Nizameev I R. Electrical properties of the gas sensing element NiO-PEDOT:PSS in a model gas mixture with nitrogen dioxide. *High Energy Chemistry*. 2024;58:S184-S188. [doi:10.1134/S0018143924700851](https://doi.org/10.1134/S0018143924700851)
36. Nizameeva G R, Lebedeva E M, Kuznetsova V V, Mansurov R N, Nizameev I R. NiO-PEDOT:PSS composite material as an active element of a conductometric sensor for nitrogen dioxide. *High Energy Chemistry*. 2024;58:S360-S365. [doi:10.1134/S0018143924701170](https://doi.org/10.1134/S0018143924701170)
37. Nizameeva G R, Nizameev I R. Anisotropic Ni-NiO network as a sensitive NO<sub>2</sub> sensor operating at room temperature. *Materials Today Communications*. 2025;42:111530. [doi:10.1016/j.mtcomm.2025.111530](https://doi.org/10.1016/j.mtcomm.2025.111530)
38. Paolucci V, Natarajan T, Ricci V, Ferrante F, Cantalini C. SnO<sub>2</sub> quantum dot decoration of CuO nanoparticles with enhanced NO<sub>2</sub> and H<sub>2</sub> gas sensing response via p-n heterojunction interfaces. *RSC Adv*. 2025;15:38750-38761. [doi:10.1039/D5RA05533D](https://doi.org/10.1039/D5RA05533D)
39. Kim YH, Kim SJ, Kim Y-J, Shim Y-S, Kim SY, Hong BH, Jang HW. Self-Activated Transparent All-Graphene Gas Sensor with Endurance to Humidity and Mechanical Bending. *ACS Nano*. 2015;9(10):10453-10460. [doi:10.1021/acsnano.5b04680](https://doi.org/10.1021/acsnano.5b04680)
40. Cho B, Yoon J, Lim SK, Kim AR, Kim D-H, Park S-G, Kwon J-D, Lee Y-J, Lee K-H, Lee BH, Ko HC, Hahn MG. Chemical Sensing of 2D Graphene/MoS<sub>2</sub> Heterostructure device. *ACS Appl Mater Inter*. 2015;7(30):16775-16780. [doi:10.1021/acscami.5b04541](https://doi.org/10.1021/acscami.5b04541)
41. Xie T, Sullivan N, Steffens K, Wen B, Liu G, Debnath R, Davydov A, Gomez R, Motayed A. UV-assisted room-temperature chemiresistive NO<sub>2</sub> sensor based on TiO<sub>2</sub> thin film. *J Allow Compd*. 2015;653:255-259. [doi:10.1016/j.jallcom.2015.09.021](https://doi.org/10.1016/j.jallcom.2015.09.021)
42. Lu G, Park S, Yu K, Ruoff R S, Ocola L E, Rosenmann D, Chen J. Toward Practical Gas Sensing with Highly Reduced Graphene Oxide: A New Signal Processing Method To Circumvent Run-to-Run and Device-to-Device Variations. *ACS Nano*. 2011;5(2):1154-1164. [doi:10.1021/nn102803q](https://doi.org/10.1021/nn102803q)
43. Navale S T, Mane A T, Chougule M A, Sakhare R D, Nalage S R, Patil V B. Highly selective and sensitive room temperature NO<sub>2</sub> gas sensor based on polypyrrole thin films. *Synthetic Metals*. 2014;189:94-99. [doi:10.1016/j.synthmet.2014.01.002](https://doi.org/10.1016/j.synthmet.2014.01.002)